Effect of the Endwall Motion on a Hydrofoil with Various Widths of Clearance

Q Guo[1, 3], L J Zhou[1, 3], Z W Wang[2], R F Xiao[1, 3], Z F Yao[1, 3]

[1] College of Water Resources and Civil Engineering, China Agricultural University, Beijing, 100083, China

[2] Department of Thermal Engineering, Tsinghua University, Beijing, 100084, China

[3] Beijing Engineering Research Center of Safety and Energy Saving Technology for Water Supply Network System, Beijing, 100083, China

E-mail: zlj@cau.edu.cn

Abstract. This paper is devoted to evaluate the effects of the relative motion between the blade tip and casing wall with different widths of gap. The steady non-cavitating simulations around a sharp tip hydrofoil in tunnel with a moving endwall are implemented and another calculation with the stationary wall is carried out as a contrast. Overall, the endwall motion moves the trajectory of the tip leakage vortex (TLV) much closer to the foil but brings small effect on the streamwise vorticity and the minimum pressure in the TLV. The influence of the gap width is taken into account with the normalized gap width within τ=0.02~0.4. The flow features on a cross section inside the gap suggest that the endwall motion causes a little lower leakage flow rate and velocity in pitchwise direction. Inside a wider gap like τ=0.2, the pressure of the tip separation vortex (TSV) is a little higher and the direction of the velocity gradient for the streamwise flow is changed under the effect of the moving wall. The foil loading characteristics are revealed by the lift and drag coefficients which are a slightly lower under the effect of the endwall motion.

1. Introduction

The clearance, or gap, between the blade tip and casing wall is indispensable in many axial flow pumps, Kaplan and bulb turbines. The tip leakage flow from the clearance will lead to efficiency losses [1] and cavitation phenomena with undesired consequences for hydraulic machines. Two typical kinds of cavitation occurring near the tip clearance are the clearance cavitation and the tip vortex cavitation [2]. The tip vortex cavitation forms in the tip leakage vortex (TLV) core and develops in the channels between the blades along the vortex trajectory. The clearance cavitation can be limited by rounding the intersections of the leading edge and the pressure side with the tip surface [3], while there are many hydraulic machines with the sharp tip edges in actual operation. The real life turbine prototypes usually tend to run with the smallest possible gap to minimize the leakage losses [4], but the influence of the gap width on the leakage vortex flow and the related cavitation features is not

quite clear. Dreyer et al. [5] experimentally investigated the TLV at the tip of a fixed hydrofoil for different confinements and flow parameters. In the test, the foil tip pressure side corner was rounded to limit the clearance cavitation during the flow visualizations, and the effect of the relative motion between the rotating blades and the casing of an axial turbine was not taken into account.

Chen [6] illustrated some conflicting evidence in literatures regarding the influence of relative wall motion. According to a relationship among some parameters near the clearance, Chen carried out an approximate analysis method to assess the significance of the relative wall motion on the clearance flow in a turbomachine. Referring to some researches on a cascade with a moving endwall system, it can be found that many critical features of the leakage vortex were almost unaffected by the endwall motion, including the streamwise mean-velocity deficit and the production of turbulence in the downstream of a linear cascade [7], but the endwall motion did distort the shape of the tip leakage vortex and displace its centre as reported in [7-8]. Moreover, Tallman and Lakshminarayana [9] showed that the casing relative motion altered the flow losses in the passage and gap. El-Batsh and Bassily Hanna [10] analysed the influence of the rotational speed on the clearance loss of an annular cascade. In the above studies of the relative wall motion, the clearance width was limited to a single or a few values.

In order to have a further understanding about the effects of the relative wall motion and gap width on the clearance vortex field, numerical simulations around a sharp tip hydrofoil in tunnel are implemented. The clearance or gap is between the fixed foil tip and a moving lateral wall of tunnel. Another simulation case without the relative motion is set as a contrast. The effects of the endwall motion with various gap widths are discussed through the analysis of the vortex features, flow field characteristics and the hydrofoil performance.

2. Methodology

2.1 Computational domain

Referring to Dreyer et al.'s experiment [5], a NACA0009 hydrofoil with a sharp tip was used as a generic blade in a water tunnel. This foil had a truncated chord (c) of 100mm, maximum thickness (h) of 9.9mm and span of 150mm. The squared test section of tunnel was 150mm wide and 750mm long. A normalized tip clearance (τ) was defined as the ratio of the gap width and h. In consideration of the dimensionless gap is typically between 0.01 and 0.1 in the normal operation of a real life turbine [4], the values of τ were set within 0.02~0.4 in present simulations.

2.2 Boundary conditions and numerical simulation

The computational domain with a moving lateral wall of tunnel shown in Figure 1(a) was used to imitate the relative motion between the rotating blade and the casing of a turbine. The boundary conditions were determined by the flow information near the blade tip of a referenced turbine, as illustrated in Figure 1(b). The relative velocity (V_{rel}) on the inlet of the blade tip was set as the tunnel inflow velocity, where the V_{rel} was a vector composition of the circular velocity (V_c) and the axial velocity (V_a). The moving velocity of the endwall could be calculated by the rotating speed (n) and the diameter of runner, and it should be noticed that the relative motion of the endwall was opposite to the rotational direction of the blade. Referring to the flow parameters in a model turbine, the boundary conditions included an inflow velocity of V_{in}=20m/s with the attack angle α=5°, the moving wall of V_{wall}=20m/s with an induced angle of 30° to the X axis, a static pressure of 0Pa on the outlet and no slip walls at the other boundaries. The simulation with the endwall motion was simply denoted as Case M and another simulation with the stationary walls was denoted as Case S.

The steady non-cavitating calculations were performed in ANSYS CFX with the Reynolds Averaged Navier-Stokes (RANS) equations implemented. The Reynolds stresses were calculated from the k-ω shear stress transport (SST) turbulence model. The high resolution scheme was used for the advection scheme. Convergence was specified as RMS residuals of 10^{-6}.

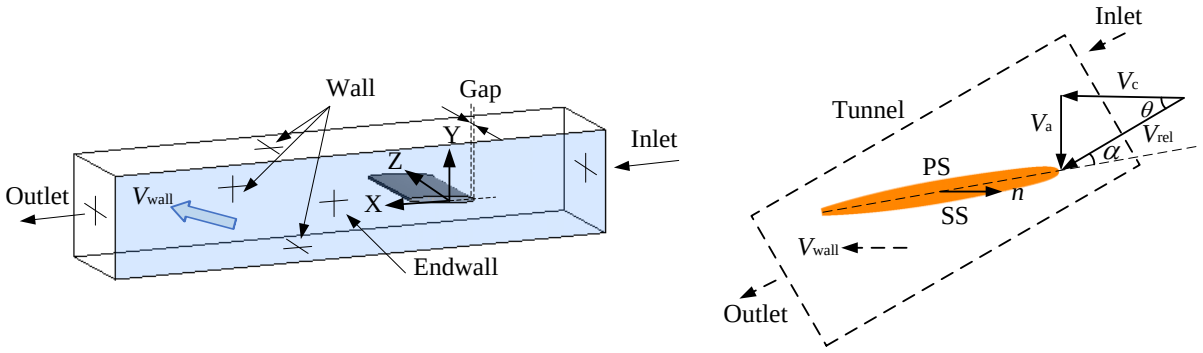

(a) Computational domain with moving endwall (b) Schematic of the blade inlet velocity

Figure 1. Computational domain and boundary conditions

2.3 Mesh generation

A structured hexahedral mesh was generated in the computational domain. The spatial resolution for measuring the downstream flow field was 0.6mm in the test [5], thus several sets of mesh element size varying from 0.8mm to 0.5mm in the corresponding region were built. The minimum pressure in the vortex centre was used as a criterion for the mesh independence check. The simulation results showed that the minimum pressure changed a little in the downstream region (x/c>0.5) but it had a significant decrease in the vicinity of foil (-0.5<x/c<0.5) with the refinement of the element size. As the low pressure is related to the cavitation, the mesh refinement was further performed in the TLV region near the foil. Under a comprehensive consideration of the computing resources, the minimum mesh size in the TLV region was about 0.15mm and the total element number was about 4.4 million finally. The wall law was used with the value of y+ on the foil profile and the both sides of the gap around 50 in average and 100 for maximum. The simulation of the final mesh has been verified in our previous work using a round tip foil with the test data [5]. Figure 2 is the partial view of the mesh near the foil tip.

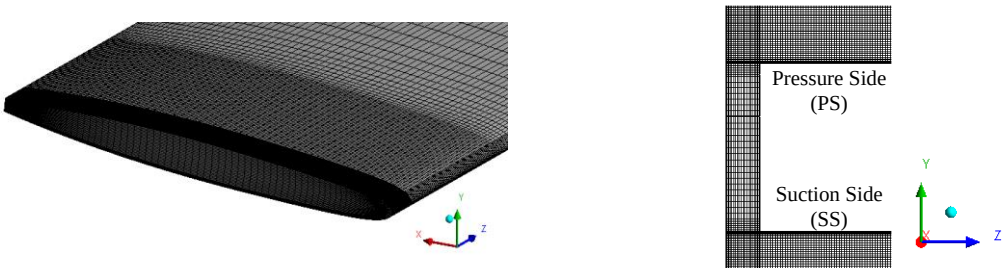

(a) Local mesh on the foil tip (b) Local mesh in the YZ plane

Figure 2. Partial view of the mesh near the foil tip

3. Results and discussion

3.1 Endwall motion effect on the tip leakage vortex

Several kinds of vortices may appear in the vicinity and downstream of the tip clearance like an induced vortex and one or further tip separation vortices (TSV) and a tip leakage vortex (TLV). The vortex visualization is shown in Figure 3 using the iso-surface of λ_2 criterion [11] coloured by the streamwise vorticity. As the rotational direction of these vortices can be determined by the velocity vector in present simulation and referred to the research in a cascade [12], it is found the TLV and

TSV has negative streamwise vorticity and the counter-rotating induced vortex has the positive streamwise vorticity in the present coordinate system. Figure 3 shows that the TLV is the dominating vortex on most conditions, the TSV is visible inside the larger gap of τ=0.4 and the induced vortex is obvious in some cases especially with the endwall motion. This section is focus primarily on the characteristics of the TLV which seems to dominate the clearance flow structure.

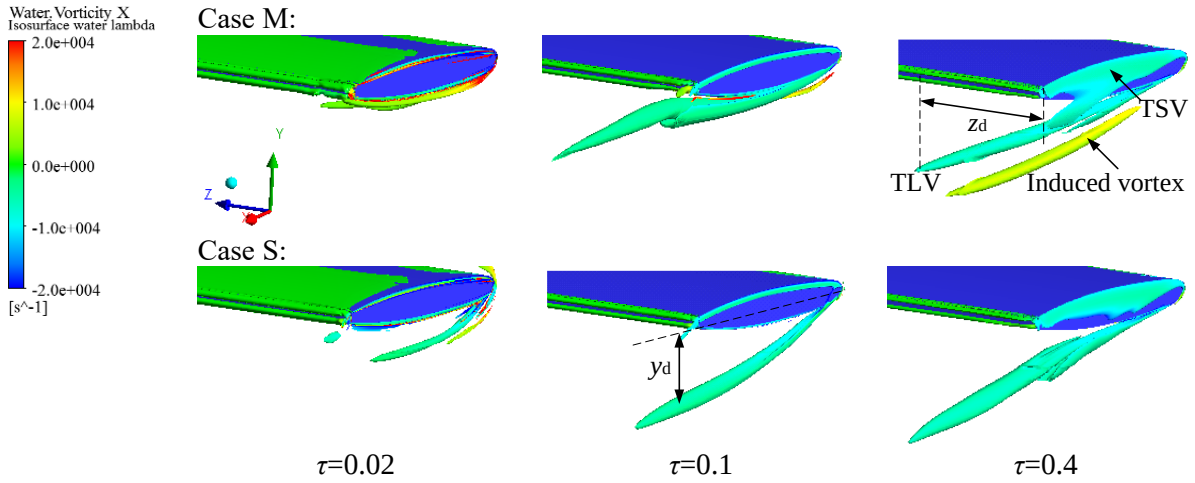

Figure 3. Tip vortices visualisation using the λ_2 criterion

Figure 4 displays the quantified trajectory of TLV with different widths of gap. The location of the vortex center is determined by the region with the maximum negative streamwise vorticity beneath the SS of foil. The horizontal axis is the streamwise position normalized by the foil chord. The pitchwise displacement (y_d) is between the vortex center and the chord line, and the spanwise location (z_d) is measured from the foil tip. The vertical axis is the parameter normalized by the chord and span of foil respectively. It can be seen that the endwall motion moves the TLV much closer to the SS and away from the gap in the spanwise direction. In Case M, the y_d of TLV is within 0.2c in the vicinity of foil, which indicates the TLV is more likely to influence the own blade than the adjacent blade unless with a very high cascade solidity in a turbine. Under the effect of the endwall motion, the TLV is shorter at τ=0.02 and it is nearly covered by the induced vortex as shown in Figure 3, meanwhile, the TLV is indeed less coherent with a short length with the narrow gap. In addition, the endwall motion significantly reduces the y_d with little change for z_d at τ=0.1 and increases the z_d a lot with little variation of y_d for the large gap at τ=0.4. It follows that the impact of the endwall motion on the trajectory of TLV has variance in different widths of gap.

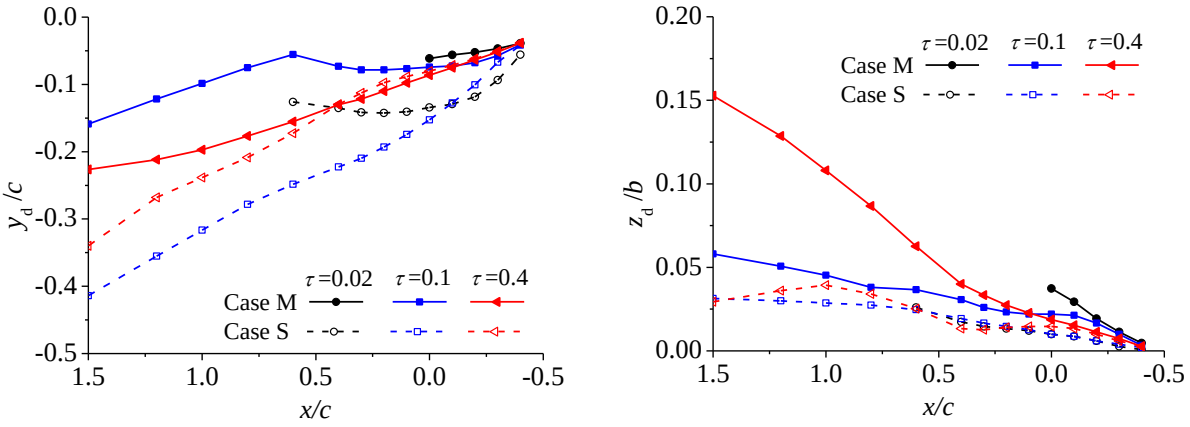

(a) Pitchwise location of TLV (b) Spanwise location of TLV

Figure 4. Trajectory of the TLV with different gap widths

Apart from the position of the vortex, the intensity of the vortex is a matter of concern. The vorticity in the vortex center can be computed from the velocity field in the test to reflect the vortex intensity, and the low pressure region which is difficult to measure in the experiment can reveal the possibility of cavitation. It is worth noting that the low pressure region also appears in the other vortices such as in the center of the distinct induced vortex at τ=0.02 and τ=0.4 in Case M, but the minimum pressure area is mainly in or very close to the core of the TLV. Therefore, the minimum pressure in the TLV becomes the main concern. Figure 5 shows the streamwise vorticity and the minimum pressure coefficient in the TLV. The minimum pressure coefficient (C_{Pmin}) is defined as

$$C_{\mathrm{Pmin}} = \frac{p_{\mathrm{ce}} - p_{\mathrm{in}}}{\frac{1}{2}\rho V_{\mathrm{in}}^2} \tag{1}$$

where the p_{ce} and p_{in} are the pressure in the TLV centre and on the inlet respectively. There is no significant difference between the Case M and Case S for the streamwise vorticity and a little difference for the C_{Pmin} in Figure 5, in spite of the significant deviation on the trajectory in Figure 4. This phenomenon can be explained by the research on a cascade that the endwall motion does not fundamentally alter the mechanisms that govern the development of the vortex's mean flow although it displaces the leakage vortex [7].

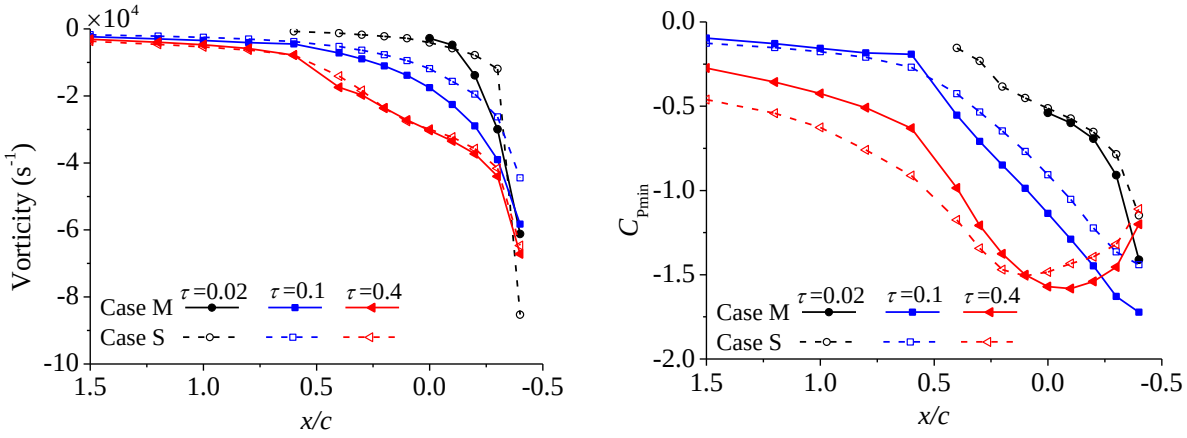

(a) Streamwise vorticity (b) Minimum pressure coefficient

Figure 5. Variation for the streamwise vorticity and minimum pressure coefficient of the TLV

With the development of TLV, the curves show a reduced magnitude of streamwise vorticity and an increased pressure in the vortex center, and there is a rapid change in the vicinity of foil with a bigger slope compared to that in the downstream. As the lower pressure in TLV with its adjacent positions to the foil may cause damage from cavitation on the SS, the measurements in a stationary tunnel especially need a certain correction to consider the effect of endwall motion on the vortex trajectory. For the narrow gap of τ=0.02, the pressure in the TLV core is higher than that with the other gap widths. From the point of view that reducing the probability and range of the cavitation, it can be speculated that the smallest possible gap used in the real life turbine is favourable. It should be noted that the gap width may increase over the operating time and then the wider gap caused by the blade tip erosion will increase the risk of cavitation with lower C_{Pmin}.

3.2 Endwall motion effect on the flow features in the gap

The tip clearance results in some leakage flow through the narrow gap, and the smallest possible gap is usually used to minimize the leakage rate and efficiency losses in a hydraulic turbine. Figure 6 shows the leakage rate (Q) and velocity (V) passing through the gap. The Q is in the pitchwise direction through a section across the gap and the V is the area-averaged velocity on this section. The vertical axis represent the variables normalized by the inflow information. It shows that the Q accounts for a

small part of the Q_{in} and the leakage velocity V occupies about half of the V_{in} due to the small area of the cross section. With the decreasing of the gap width, the value of Q is reducing as expected and the V is increasing until to τ=0.05 and then decreases. Under the effect of the endwall motion, the Q and V is a little lower than that in the Case S.

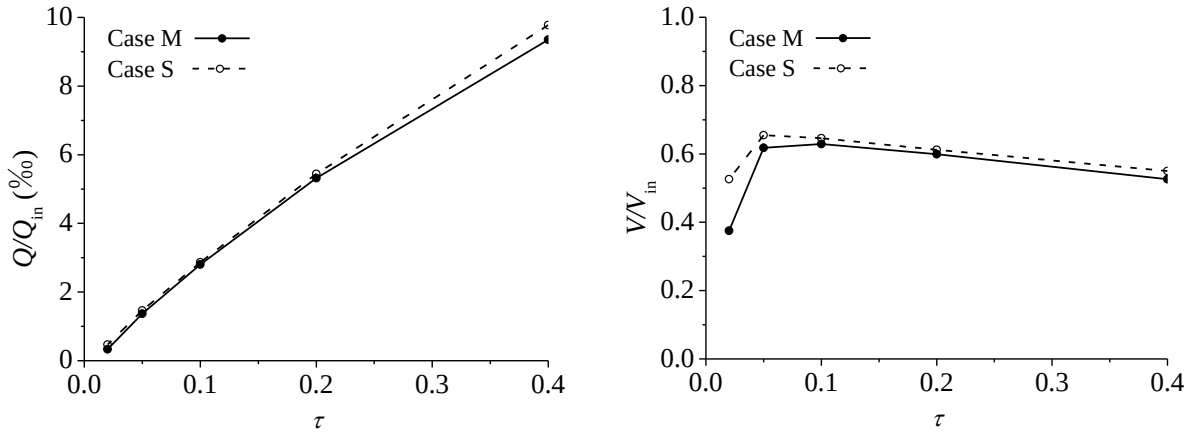

(a) Non-dimensional leakage flow rate (b) Non-dimensional average velocity

Figure 6. Variation of the leakage flow rate and velocity through the clearance

The TSV inside the gap will add the complexity in the clearance. The present simulation gets the TSV in the wider gap at τ=0.2 and τ=0.4 as this vortex is barely developed for the smallest gap [13]. In order to investigate the effect of the endwall motion, the flow features in the gap with two typical widths of τ=0.2 and τ=0.05 with and without the TSV respectively are analysed. As the TSV originally appears near the forepart region inside gap, Figure 7 shows the pressure distribution on a streamwise plane of x/c=-0.4 in both cases. Under the effect of the endwall motion, the pressure is a little higher inside the gap especially in the TSV core at τ=0.2. On the contrary, the TLV has a lower pressure center with the endwall motion near the forepart of foil as illustrated in Figure 5(b). In consideration of the possibility of the cavitation, the endwall motion reduces the clearance cavitation but aggravates the leakage vortex cavitation in the vicinity of foil.

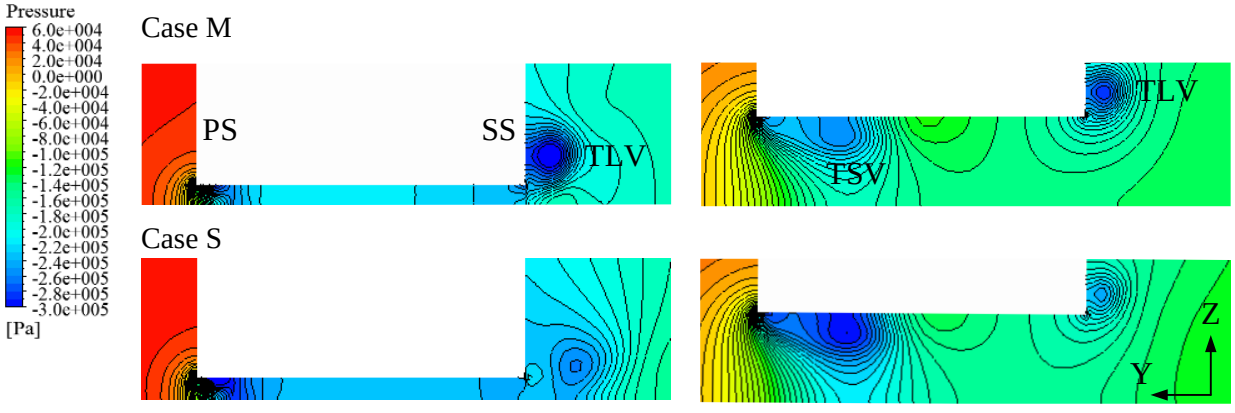

(a) τ=0.05 (b) τ=0.2

Figure 7. Pressure distribution on the streamwise plane of x/c=-0.4

Figure 8 and Figure 9 display the distribution of the streamwise and pitchwise velocities on the plane of x/c=-0.4. The pressure difference across the blade tip creates the clearance flow through the gap from the PS to SS of foil and the pitchwise motion of the clearance flow is embodied by the large value of the negative Y axial velocity in the gap. The pitchwise flow is relatively uniform in the small gap at τ=0.05 but the flow separation appears at the PS corner when τ=0.2 with some changes of the

pitchwise velocity near the TSV region. In Figure 8, the relative motion changes the velocity gradient which is mainly along Z axial direction in the Case N but in Y-direction in Case M. It is speculated that the viscous effect of the static wall plays a major role in the Case S and makes the velocity gradient is normal to the wall. In Case M, the moving endwall with a velocity component $V_{\text{wall-y}}$ weakens the viscous effect but this phenomenon is less obvious in the narrower gap due to the much confinement from the two side walls of the gap.

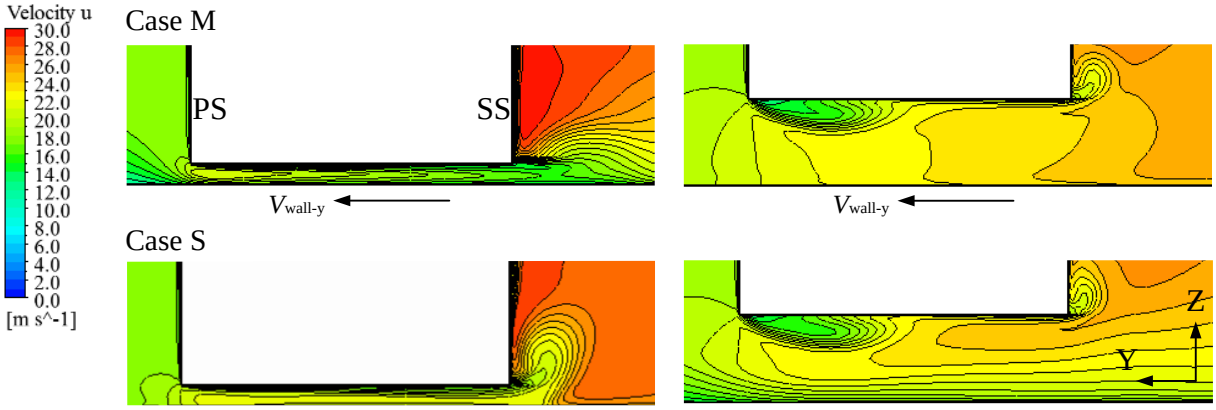

(a) τ=0.05 (b) τ=0.2

Figure 8. Streamwise velocity distribution on the plane of x/c=-0.4

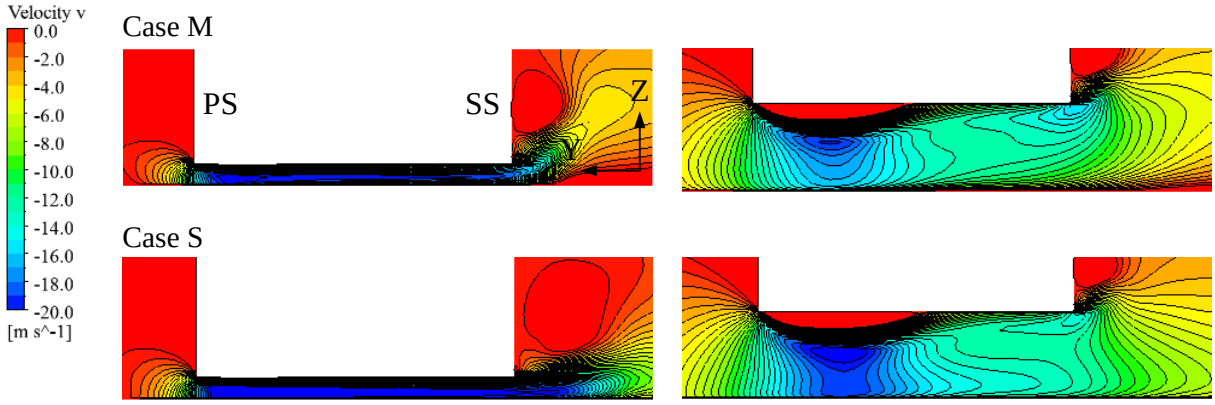

(a) τ=0.05 (b) τ=0.2

Figure 9. Pitchwise velocity distribution on the plane of x/c=-0.4

3.3 Endwall motion effect on the foil loading characteristics

The foil loading characteristics can be analysed through the non-dimensional lift and drag coefficients (C_L and C_D), which are defined as

$$C_L = \frac{L}{\frac{1}{2}\rho V_{\text{in}}^2 cb} \tag{2}$$

$$C_D = \frac{D}{\frac{1}{2}\rho V_{\text{in}}^2 cb} \tag{3}$$

where L and D represent the lift and drag forces normal and parallel to the inflow, which are the forces in Y and Z axial directions in present simulation, and b is the effective span of the foil in tunnel depending on the gap width. Figure 10 shows the variation of C_L and C_D with the gap width in both

cases. With the increasing of the τ, the C_L decreases gradually and the relatively small C_D increases slightly. Generally speaking, with the increasing of the blade tip clearance for a turbine, the efficiency losses will increase. The reduced lift coefficient will directly affect the torque of runner and then the power. The effect of the endwall motion leads to a slightly lower C_L and C_D with little change for the foil loading characteristics.

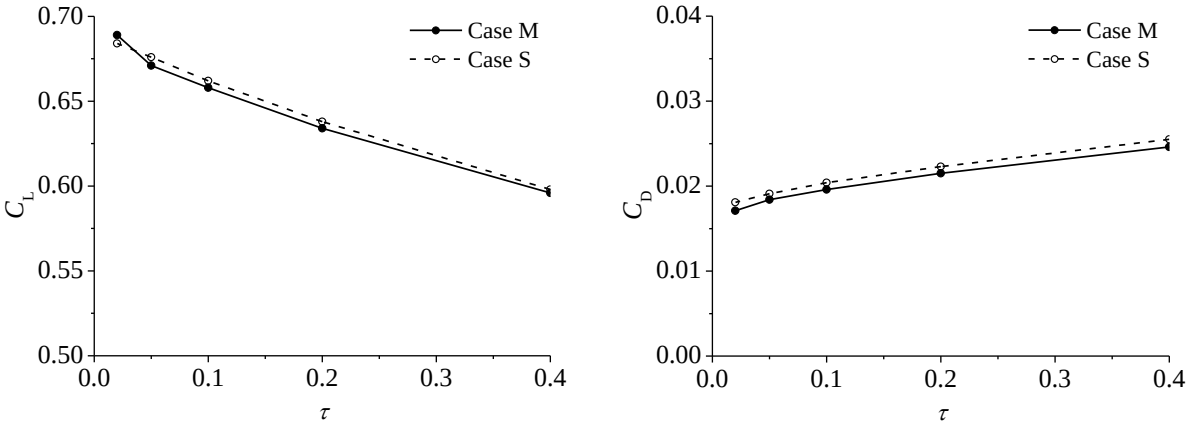

(a) Lift coefficient (b) Drag coefficient

Figure 10. Variation of the lift and drag coefficients

4. Conclusions

The tip clearance flow around a sharp tip hydrofoil was simulated with and without the moving endwall to investigate the effect of the relative wall motion. The influence of the gap width was taken into consideration within τ=0.02~0.4. Some observations made as results are as follows.

(1) In general, the tip leakage vortex (TLV) is the dominating vortex with the minimum pressure in the clearance flow field. Under the effect of the endwall motion, the trajectory of the TLV is much closer to the foil suction side and away from the gap in the spanwise direction. The endwall motion brings small impact for the streamwise vorticity and the minimum pressure in the TLV core. With the different widths of gap, the trajectory and pressure of TLV is influenced by the moving endwall in different degree.

(2) The endwall motion makes a little lower leakage flow rate and flow velocity through the gap. On a streamwise plane near the foil forepart, the moving endwall leads to a little higher pressure in the tip separation vortex (TSV) and a bit lower pressure in TLV. The direction of the velocity gradient for the streamwise flow is changed obviously by the endwall motion especially in a wider gap like τ=0.2.

(3) The foil loading characteristics is reflected by the lift and drag coefficients (C_L and C_D). The endwall motion leads to a slightly lower C_L and C_D.

Acknowledgements

The authors thank the National Natural Science Foundation of China (Nos. 51279205 and 51479200) for supporting this work.

References

[1] Booth T C, Dodge P R and Hepworth H K 1982 *J. Eng Power* **104** 154-161
[2] Laborde R, Chantrel P and Mory M 1997 *J. Fluids Eng Trans ASME* **119** 680-685
[3] Gearhart W S 1966 *J. Aircraft* **3** 185-192
[4] Dreyer M, Decaix J, Münch-Alligné C and Farhat M 2014 *IOP Conf. Ser. Earth Environ. Sci.* **22** 1-7
[5] Dreyer M, Decaix J, Münch-Alligné C and Farhat M 2014 *Exp Fluids* **55** 1-13
[6] Chen G T 1991 *Massachusetts Institute of Technology*
[7] Wang Y and Devenport W J 2004 *AIAA J* **42** 2332-2340
[8] Palafox P, LaGraff J E, Oldfield M L G and Jones T V 2005 *Proc. ASME Turbo Expo* **6** 465-476

[9] Tallman J and Lakshminarayana B 2001 *J. Turbomach.* **123** 324-333
[10] El-Batsh H M and Bassily Hanna M 2011 *Int. J. Rotating Machinery* **2011** 489150
[11] Jeong J and Hussain F 1995 *J. Fluid Mech.* **285** 69-94
[12] You D, Wang M, Moin P and Mittal R 2007 *J. Fluid Mech.* **586** 177-204
[13] Decaix J, Balarac G, Dreyer M, Farhat M and Münch C 2015 *Journal of Turbulence* **16** 309-341